Published in: Seventh International Conference on Indoor Positioning and Indoor Navigation (IPIN), Alcala de Henares, Madrid, Spain, October, 2016.
http://dx.doi.org/10.1109/IPIN.2016.7743696

Multi-User Interference and Wireless Clock Synchronization in TDOA-based UWB Localization

Janis Tiemann, Fabian Eckermann and Christian Wietfeld
TU Dortmund University, Communication Networks Institute (CNI)
Otto-Hahn-Str. 6, 44227 Dortmund, Germany
{janis.tiemann, fabian.eckermann and christian.wietfeld}@tu-dortmund.de

***Abstract*—Wireless positioning based on IEEE 802.15.4a has recently gained attention for precise localization. However, the multi-user scalability of those, mostly two-way ranging based, approaches is not considered. Due to the exchange of multiple frames per ranging, two-way ranging has significant downsides in terms of scalability. This paper proposes and validates a novel multi-user time-difference of arrival based localization approach using wireless clock synchronization to overcome the limitations of two-way ranging based positioning. The clock characteristics of the individual nodes are experimentally analyzed and the requirements and constraints for wireless clock synchronization are elaborated based on the experiments. The results show, that a clock synchronization rate of around 1 Hz is sufficient to achieve accuracies in the decimeter range. Experiments analyzing the multi-user capabilities of the system are conducted, highlighting the specific properties of multi-user access in the proposed time-difference of arrival based localization. The experiments show, that the system is capable of scaling gracefully under heavy load. However, clock synchronization suffers as it is degrading equally. Therefore, a novel approach is proposed and evaluated to prioritize the wireless clock synchronization to ensure load independent positioning accuracy. It is shown, that the proposed approach is capable of ensuring a synchronization receive ratio of around 90 % independent of the system load.**

***Keywords*—Ultra-wideband (UWB), Time-Difference of Arrival (TDOA), Wireless Clock Synchronization, Wireless Sensor Network, Indoor-Positioning, Channel Access.**

I. Introduction and Related Work

The research and usage of modern ultra-wideband (UWB) IEEE 802.15.4a based localization was enabled recently by newly available integrated transceivers. The ease of use, degree of integration and therefore the comparably low pricepoint challenged a lot of research [1]. UWB based systems are used to enable indoor unmanned autonomous vehicle (UAV) navigation [2], for autonomous driving in global navigation satellite system (GNSS) denied environments [3] and for GNSS augmentation and ambiguity resolution [4]. Most of the above research achieves decimeter accuracies [5], strongly depending on the amount over anchor nodes, the used constellation and environment specific multipath effects [6]. However, most of this research focuses on constrained scenarios. Mostly, just a single node is localized in a given set of anchors using two-way ranging (TWR) or symmetric double-sided two-way ranging (SDS-TWR). The use of two-way ranging has the advantage of a simple system topology, as the communication is directly resulting in a range that can directly be used for position estimation. In most cases this is sufficient due to the lack of multi-user interference, as only one node is positioning itself. However, for practical system, especially in industrial environments, more participants are to be localized, see Fig. 1. Since TWR uses at least the exchange of two messages per range [7] and SDS-TWR uses three to four frames [8], the channel usage is increasing proportionally with the amount of anchors [9]. This becomes even worse when TWR is conducted without any form of channel sensing or central coordination, as the reception of a single interfering message destroys a complete ranging procedure due to the critical inter-frame timings. Next to the channel usage, energy consumption of TWR based positioning is preventing self contained, long-term battery powered nodes that may depend on power from energy harvesting.

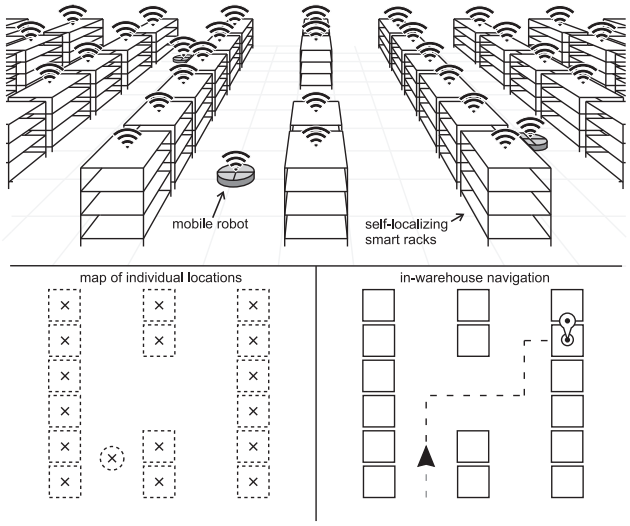

Fig. 1. Illustration of an industrial scenario where multiple robots are organizing a warehouse. In order to find the goods, a central organization unit keeps track of the robots as well as the goods position. Note that the massive use of wireless localization is challenging the channel capabilities..

Therefore, to overcome those problems, this paper presents a time-difference of arrival (TDOA) based approach with wireless clock synchronization for IEEE 802.15.4a based UWB systems. The transmission of single frame is required to localize a tag node within the system. TDOA requires synchronized clocks. In contrast to many commercial systems [10], this paper implements wireless clock synchronization through a synchronization node. The basic concept for clock synchronization used in this paper is not new. In [11] a static two-dimensional RTLS with three anchors and a single tag is proposed using TDOA with wireless clock synchronization.

978-1-5090-2425-4/16/$31.00

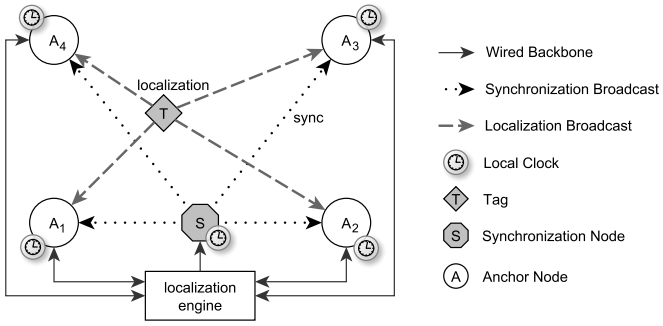

Fig. 2. Topology of the TDOA based localization system. The synchronization node is periodically transmitting a sync packet. The anchor nodes receive this broadcast and communicate the received timestamps to the localization engine. Note that the wired backbone is not distributing a common clock.

The proposed system is experimentally evaluated, achieving an accuracy in the range of several meters. [12] proposes wireless clock synchronization using a two-way message exchange, focusing on the mitigation of multipath effects. Joint clock skew and position estimation is theoretically investigated through simulations by [13]. Two suitable suboptimal estimators are proposed to attain the Cramér-Rao lower bound. A wireless clock synchronization and positioning experiment has been conducted in [14]. The experimental system is similar to the one used in this work. In terms of positioning accuracy, comparable results are achieved. However, an experimental analysis of multi-user interference and scalability has, best to the authors knowledge, not yet been conducted. In this work, a practical TDOA system based on IEEE 802.15.4a based hardware is implemented and evaluated. The system's properties, influencing the positioning accuracy as well as the mutli-user scalability, are theoretically and experimentally assessed. Furthermore, a novel method for wireless clock synchronization priorization is proposed and the effects on the quality of service are evaluated.

II. TDOA Positioning System Concept

The concept of TDOA positioning is most known through Global Navigation Satellite Systems (GNSS). In GNSS the satellites are transmitting precisely timed signals simultaneously. Those signals are transmitted using direct-sequence spread-spectrum with specialized pseudonoise (PN) code symbols. Those symbols have minimal cross-correlation and near-optimal auto-correlation properties, allowing for simultaneous transmission and reception. A typical GNSS receiver has multiple reception units in which, through code-correlation, the time-differences of the received signals can be estimated. In order for the system to work, an extensive ground-station network is operated that precisely tracks the satellites with laser ranging and synchronizes the space-based local clocks with more precise ground-based clocks to compensate for local clock drifts.

Since the IEEE 802.15.4a UWB physical layer (PHY) uses Burst-Position Modulation with Binary Phase-Shift Keying, receiving UWB signals is significantly more energy extensive than GNSS reception. Therefore the system topology is reversed as depicted in Fig. 2.

A. System Topology

The topology of the proposed system features a set of anchor nodes A, a synchronization node S, a localization engine and a set of tags T, that are to be localized. The anchor nodes are connected to the localization engine via a wired backbone. This wired connection may be a combination of multiple technologies and is not timing-critical. The synchronization node is periodically broadcasting a synchronization packet, precisely timed by it's local clock. The anchor nodes receive this packet and communicate the reception timestamp of the synchronization packet. This reception timestamp is timed on the local clock of the receiving node. Through this synchronization, further described in section II-B, the drift of the local clock of an anchor node is compensated by the localization engine. Due to this synchronization a single broadcast of a tag is sufficient to estimate it's position with TDOA positioning.

B. Clock Synchronization

Similar to GNSS, one of the most important aspects of TDOA positioning is the synchronization of the clocks. However, in contrast to a GNSS, not the transmitter clocks are synchronized, but the receiver clocks need to be. Therefore a wireless clock synchronization, similar to [14] is proposed. A synchronization node is transmitting a precisely timed periodic synchronization frame with the frequency f_s. The timing increment of the synchronization frame is set by the localization engine. All anchor nodes receive this synchronization frame and communicate the timestamps of the reception of their local clocks to the localization engine over the wired backbone. Through the knowledge of the timing increment, the localization engine is able to reconstruct the synchronization node's clock as a reference clock. This method requires no state or calculation on the anchor nodes themselfes.

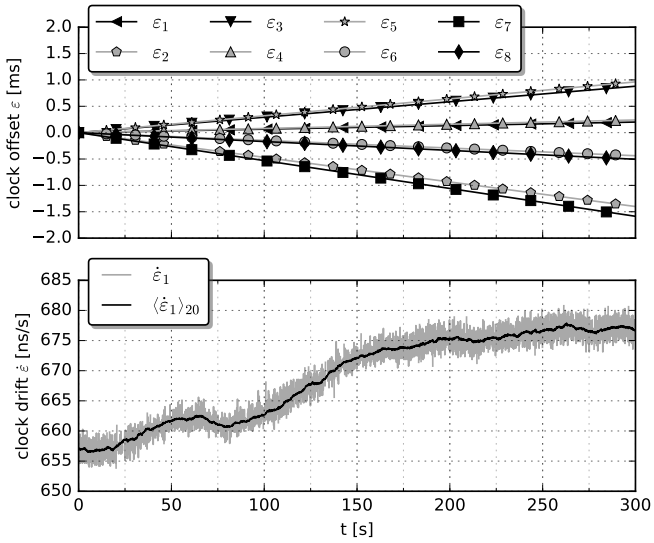

Fig. 3. Experimental evaluation of the clock offset ε for the eight anchors used in the positioning scenario. The clock drift of the first anchor $\dot{\varepsilon}_1$ is depicted below to show the effects of noise during reception and drift development. Note that the clock of the synchronization node acts as the reference clock.

To evaluate the basic clock drift, a static experiment with eight anchor nodes is conducted. Fig. 3 depicts the development of the clock offset ε of all eight individual clocks over a period of $5\,\mathrm{min}$. An almost linear behaviour is observed, with a drift from $0.25\,\mathrm{ms}$ to $1.5\,\mathrm{ms}$ over the experiment duration. This illustrates the need for clock synchronization as $1.5\,\mathrm{ms}$ corresponds with $450\,\mathrm{km}$ over the speed of light. However, the examplary analysis of the derivation of ε, the clock drift $\dot{\varepsilon}_1$ shows, that the drift is by far not linear. This is obvious as crystal oscillators are highly dependent on temperature and other environmental influences.

$$\varepsilon_{n,k} = t_{sn,k} - t_{r,k} \qquad \dot{\varepsilon}_{n,k} = (\varepsilon_{n,k} - \varepsilon_{n,k-1}) f_s \tag{1}$$

In order to obtain a common clock base for all anchors, the localization engine keeps track of ε_n and $\dot{\varepsilon}_n$ for each anchor n at a synchronization step k, see (1). When a localization frame is observed by a set of anchors, the local clock offsets are eliminated using the last obtained synchronization frame $t_{sn,k}$. Since the local clocks of the anchor nodes drift in the time between the reception of the last synchronization frame and the localization frame i, this drift has to be accounted for. Assuming a clock drift as measured in Fig. 3 of around $650\,\mathrm{ns/s}$ and a synchronization rate of f_s $=10\,\mathrm{Hz}$, the intersynchronization drift is in the range of $20\,\mathrm{m}$. Therefore, extrapolation is needed based on the last observed clock drift $\dot{\varepsilon}_{n,k}$. The drift correction $\varepsilon_{n,i}$ for the local time at each anchor is calculated in (2).

$$\varepsilon_{n,i} = \varepsilon_{n,k} + \dot{\varepsilon}_{n,k}(t_{n,i} - t_{sn,k}) \tag{2}$$

C. Positioning Method

The position is estimated by a closed form system of equations represented in matrix form by (3), see [15].

$$P_e = (A^T A)^{-1} A^T (b_1 + b_2 d_1) \tag{3}$$

With:

$$A = \begin{bmatrix} x_1 - x_i & y_1 - y_i & z_1 - z_i \\ \vdots & \vdots & \vdots \\ x_1 - x_n & y_1 - y_n & z_1 - z_n \end{bmatrix} \tag{4}$$

$$b_1 = \frac{1}{2} \begin{bmatrix} x_1^2 - x_i^2 + y_1^2 - y_i^2 + z_1^2 - z_i^2 + \Delta d_{i,1}^2 \\ \vdots \\ x_1^2 - x_n^2 + y_1^2 - y_n^2 + z_1^2 - z_n^2 + \Delta d_{n,1}^2 \end{bmatrix} \tag{5}$$

$$b_2 = \begin{bmatrix} \Delta d_{i,1} \\ \vdots \\ \Delta d_{n,1} \end{bmatrix}, \; P_e = \begin{bmatrix} x_e \\ y_e \\ z_e \end{bmatrix} \tag{6}$$

Where $x_1 ... x_n, y_1 ... y_n, z_1 ... z_n$ are the coordinates of the anchors and (x_e, y_e, z_e) the tag's estimated position, with $i = 2..n$ for n anchors. Δd is the TDOA multiplied by the speed of light. The estimated position P_e is dependent on the unknown distance to the reference anchor d_1. As the gained position lies on a sphere with the radius d_1 around the reference anchor, d_1 is obtained by solving the sphere equation described by (7).

$$(x_1 - x_e)^2 + (y_1 - y_e)^2 + (z_1 - z_e)^2 = d_1^2 \tag{7}$$

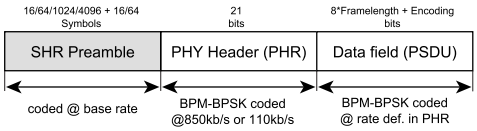

Fig. 4. Basic structure of a IEEE 802.15.4a UWB PHY frame (PPDU), see [16]. Note that a significant amount of the frame duration is taken by the synchronization header (SHR), as the data field is typically short for localization applications.

D. Channel Access and Scalability

To quantify and analyze the scalability of the TDOA based positioning system introduced in section II-A, the properties of the UWB PHY as defined in IEEE 802.15.4a-2011 have to be considered. The PHY protocol data unit (PPDU) consists of three parts: the synchronization header (SHR), the PHY header (PHR) and data field as shown by Fig. 4. Due to the wide bandwidth and the result low transmission power, the UWB signal is rather difficult to detect for the receiver. This results in the need for a rather large preamble in the SHR, such that the receiver is able to synchronize to the PPDU. This synchronization is not only important for accurate TOA estimation, but is also the basis for finding and decoding the frame itself.

The modulation scheme used is Burst-Position Modulation with Binary Phase-Shift Keying (BPM-BPSK). BPSK is widely known, whereas BPM is a special form of the popular Pulse Position Modulation. In contrast to PPM, in the UWB PHY a burst consists of a series of chips that are repeated with a known spreading code. The structure of a UWB PHY symbol is depicted in Fig. 5. The information of the symbol is then coded through the position of the burst in the possible burst position slots. A guard interval is inserted to avoid inter-symbol interference through multi-path. Since precise synchronization is needed to decode BPM-BPSK signals and due to the fact that only a small portion of the time is actually taken by a burst $T_{burst} << T_{BPM}$, the UWB PHY has rather interesting

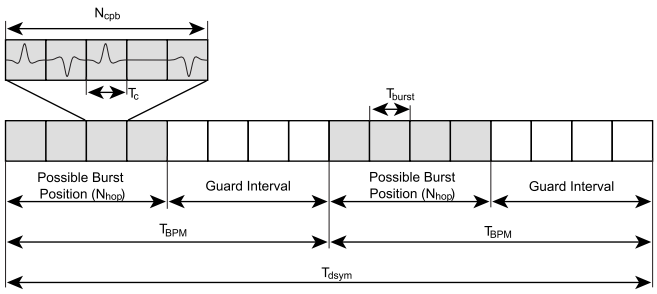

Fig. 5. Modulation scheme for a single symbol using BPM-BPSK as defined in [16]. Note a burst is only occupying a small portion of T_{dsym}.

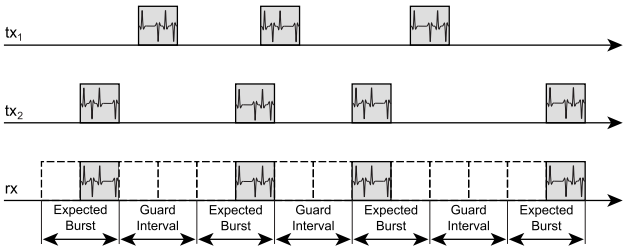

Fig. 6. Illustration of a simulataneous transmission of two UWB frames. Note that, although the first sender is sending at the same time as the second, only the second is seen by the receiver as the correlation with the reference bursts is only successful if synchronized.

multiuser interference rejection capabilities [16]. A conceptual time sequence chart of the reception of a UWB frame with potentially interfering frames is depicted in Fig. 6. It should be noted, that in the actual UWB PHY the possible burst positions are $N_{burst} = 8, 32, 128$, reducing the probability of burst collisions significantly. Another aspect is that the correlation with the reference symbol is only successful, if the received signal is precisely synchronized through the SHR. Therefore out of sync bursts have much less potential to interfere with the synchronized bursts. In order to quantify the scalability with as few as ten tags, the most challenging channel configuration for the UWB PHY was chosen. The goal is to focus on the channel and multi-user interference, therefore the maximum preamble length n_{pr} and the lowest data rate R was chosen as listed in Tab. I. The resulting durations of the SHR T_{shr}, the PHR T_{phr} and the data T_{data} of the PPDU T_{ppdu} with the symbol duration T_{dsym} are listed in Tab. II. The channel is randomly accessed without channel sensing. The time between transmissions t_n is uniformly distributed and centered around the mean channel access frequency, and bounded by $0.5/f_n < t_n < 1.5/f_n$.

E. Proposed Synchronization CDMA

Since the positioning accuracy is closely related to the successful reception of synchronization packets, which will be proven in section III-A, special effort in prioritizing synchronization packets is proposed, to ensure precise positioning under heavy system load. Therefore, a novel approach is proposed to ensure a certain quality of service for synchronization frames. The synchronization code division multiple access (SyncCDMA) approach is offloading the synchronization frames to a different preamble spreading code. The anchors switch their receivers to the synchronization code within defined intervals after successful sync frame reception. However, through the switching process and the use of certain margins, the receiver is unable to receive localization frames for a certain timeframe. This is expected to have an effect

TABLE I. CHANNEL CONFIGURATION USED IN THE EXPERIMENTS.

f_c [GHz]	B [MHz]	n_{prc}	f_{pr} [MHz]	R [kbps]	c_{pr}	n_{pr}
6.4896	499.2	127	62.4	110	9	4096

TABLE II. TEMPORAL PPDU COMPOSITION OF UWB FRAMES.

T_{ppdu} [ms]	T_{shr} [ms]	T_{phr} [ms]	T_{data} [ms]	T_{dsym} [μs]
5.7764	4.4226	0.1723	1.1815	8.205

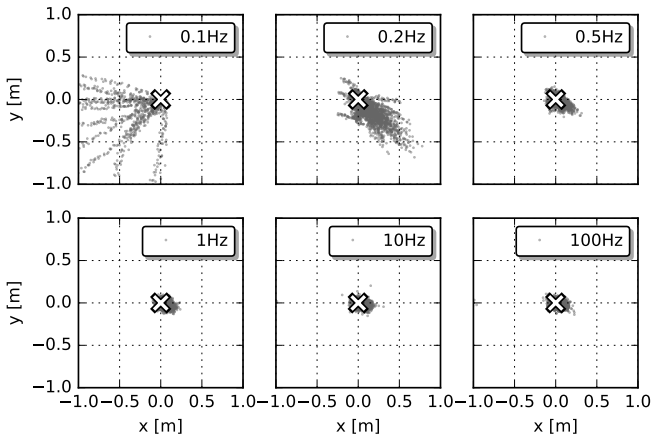

Fig. 7. Experimental results of TDOA positioning with wireless clock synchronization. A static position is evaluated using positioning with a variation of synchronization frequencies. Note that as expected, the variation in the positioning error is decreasing as the synchronization frequency increases.

on the overall reception rate, resulting in a trade-off between positioning accuracy and update frequency.

III. EXPERIMENTAL RESULTS

A set of experiments was conducted to evaluate the proposed TDOA system. The dependency of the positioning accuracy on the synchronization rate, as well as the scalability and quality of service are analyzed. For traceability, reproducibility and comparability, the raw data is published alongside this work [17].

A. Synchronization Rate vs. Positioning Accuracy

To qualitatively analyze the dependency of the positioning error on the synchronization rate, a static positioning experiment is conducted. A set of eight anchors is placed in a laboratory setup. The anchor positions are published along with the raw data [17]. The tag that is to be localized, is located in the center of the constellation at $p_t = [0, 0, 0.18]$. The position of the tag, as well as the position of the anchors were measured using a line laser system. However, the absolute accuracy is not in the center of this work. Therefore, only a single position and orientation is evaluated.

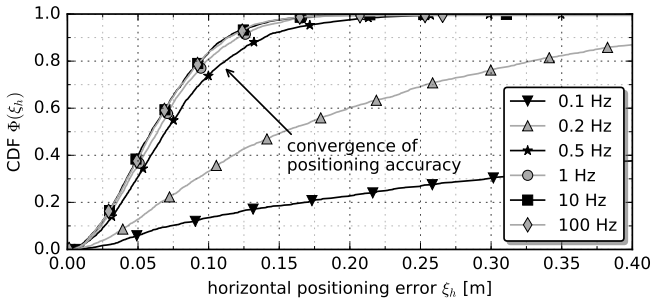

Fig. 8. Error analysis for different synchronization frequencies of the TDOA positioning experiment. Note that the error is slightly increasing again at 100 Hz. This is expected to be related to the unfiltered clock drift extrapolation used in the evaluation.

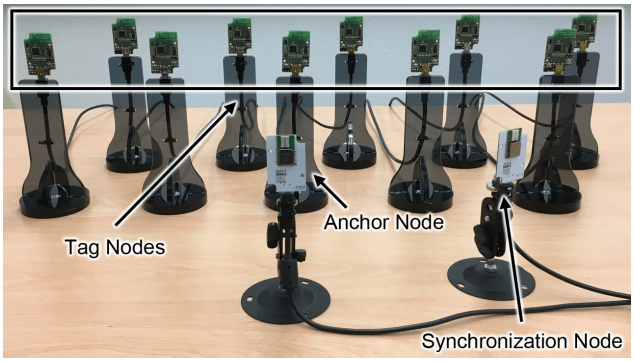

Fig. 9. Experimental setup to analyze the scalability in terms of multi-user interference. Ten tag nodes, an anchor node and a synchronization node were used. Note that only one anchor node was used to get consistent results.

The two-dimensional positioning results of this experiment are depicted in Fig. 7. The synchronization frequency was varied from $0.1\,\mathrm{Hz}$ to $100\,\mathrm{Hz}$. The errors caused by a low synchronization rate are most visible at $0.1\,\mathrm{Hz}$. The resulting positions drift along a set of lines, as the individual clocks drift over the unsynchronized timeframes. This effect is decreasing with an increasing synchronization rate. To quantify this effect, the cumulated distribution functions (CDF) of the horizontal positioning error are analyzed as depicted in Fig. 8. The CDFs for synchronization rates under $1\,\mathrm{Hz}$ are significantly lower than the ones over $1\,\mathrm{Hz}$, which are rather close to each other. Assuming the scenario that was experimentally analyzed, a frequency of $\sim 1\,\mathrm{Hz}$ appears sufficient for basic anchor clock synchronization.

B. Scalability Analysis

To quantify the effect of multi-user channel access, another experiment is conducted. The experimental setup is depicted in Fig. 9. A set of ten tag nodes is placed, facing an anchor node and a synchronization node. The tags transmit frames using a randomly chosen inter-frame time with a defined mean frequency f_n. The anchor is receiving those frames and reporting them to the localization engine which then records frame reception. The transmission receive ratio was validated using a logic analyzer on each tag and the anchor itself simultaneously. In order to achieve channel saturation, minimize computation times in the microcontroller and the limitations of the wired backbone, the maximum frame-length was chosen. One experiment with random access and no differentiation in the anchor and another one with SyncCDMA, as proposed in section II-E, is conducted.

The results of the experiments are depicted in Fig. 10. As a reference, the typical pure ALOHA [18] curve assuming destructive frame collisions is shown. Also, the maximum throughput when assuming that a frame can only be received with full preamble is shown through $1/T_{ppdu}$. The results show, that neither apply to the UWB PHY channel, which is due to the physical properties of UWB transmissions outlined in section II-D. The received frames do not suffer from traditional destructive frame collision, but from pulse collision, which has a significantly smaller effect. Also, more frames than $1/T_{ppdu}$ are received. Although it may seem counter-intuitive first, most of the time in the PPDU is taken by the preamble. Frame reception however, requires only a small part

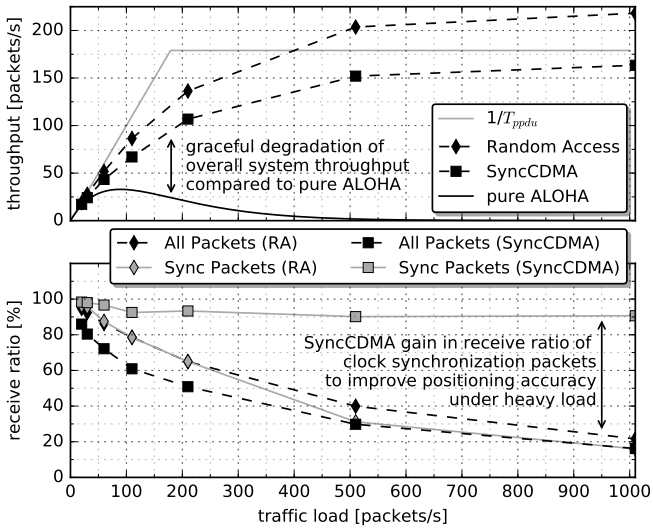

Fig. 10. Experimental results of the scalability analysis. The results for random access and the throughput using SyncCDMA are shown. A typical pure ALOHA curve with destructive frame collision is shown. Note that the worst-case channel configuration with the longest frame duration was used.

of the SHR for successful synchronization at a low distance. Therefore, both effect show, that in terms of throughput, the UWB physical layer is capable of natively scaling to heavy traffic on the shared medium, degrading gracefully.

However, when looking at the receive ratio, this corresponds with the ratio of successfully received frames. All frames are treated equally as there is no possibility to differentiate before PHR reception. Therefore also the receive ratio of synchronization frames drops, resulting in significant degradation of the positioning accuracy, as shown by section III-A. In order to counter this effect, a method to offload synchronization frames to a different spreading code is proposed in section II-E. The results show clearly, that through this method the receive ratio for synchronization frames may be held at at least $90\,\%$ for all different tested traffic loads. However, the overall throughput as well as the receive ratio are decreasing slightly with SyncCDMA. This is due to the margins needed to ensure reliable reception of synchronization frames.

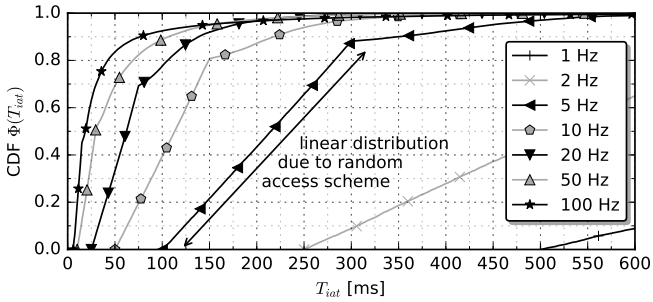

Fig. 11. Cummulative distribution functions $\Phi(T_{iat})$ of the experimentally measured inter-arrival times T_{iat} for a single tag in the multi-tag setup. Note that the linear distributed area is caused by the random access scheme.

C. Quality of Service Analysis

Next to the throughput and the receive ratio another important metric for the analysis of localization systems is the achievable quality of service for the inter-arrival times (IAT). To analyse which T_{iat} can be expected, the results of the experiment conducted in section III-B are analyzed. The CDFs $\Phi(T_{iat})$ for different mean localization frequencies f_n are depicted in Fig. 11. Note that T_{iat} is representing the time between two positioning samples of a single tag. The CDFs show a linear part, that is caused by the random access procedure described in section II-D. However, the size of the linear part decreases with increasing channel utilization, most visible at around $f_n = 100\ Hz$. This effect shows, that the expected quality of service strongly depends on the channel utilization. However, using a random access scheme, inter-arrival times in the range of $1/f_n$ cannot be guaranteed.

It should be noted, that the used channel configuration is focusing on the worst case scenario with the longest possible T_{ppdu} defined in [16]. This configuration is chosen to neglect side-effects like processing time in the used microcontroller unit, backbone limitations of the current setup and to analyze multi-user interference with a practical amount of tags. However, in terms of multi-user scaling though, much higher positioning frequencies are possible through other preamble lengths and data rates.

IV. Conclusion

This paper introduces a practical UWB based system using TDOA for localization to achieve higher update rates and lower power consumption at the tag itself. Wireless clock synchronization is implemented to distribute a common timebase to the anchors. The effect of the synchronization frequency on the localization accuracy is experimentally evaluated. A novel method to ensure a stable clock synchronization under high system loads is introduced and experimentally assessed. The multi-user interference and therefore the systems capability is theoretically and experimentally evaluated, showing that TDOA based systems degrade gracefully under increasing load due to the modulation scheme of UWB as defined in [16]. The positioning quality of service in terms of inter-arrival times is evaluated experimentally per individual tag. It is demonstrated that, although a random channel access is conducted, the system is capable of delivering high update rates.

Future work may include a detailed analytical and experimental comparison between TDOA and TWR based systems in terms of multi-user scalability. Another aspect that may exploit the specific needs in localization may be the design of a scheduled access scheme precisely tailored for multi-user application, graceful scaling and guaranteed quality of service.

Acknowledgement

The work on this paper has been partially funded by Deutsche Forschungsgemeinschaft (DFG) within the Collaborative Research Center SFB 876 “Providing Information by Resource-Constrained Analysis”, project A4 and has received funding from the federal state of Northrhine-Westphalia and the “European Regional Development Fund” (EFRE) 2014-202 in the course of the “CPS.HUB/NRW” project under grant number EFRE-0400008.

References

[1] B. Silva, Z Pang, J. Akerberg, J. Neander, and G. Hancke. Experimental study of UWB-based high precision localization for industrial applications. In *Ultra-WideBand (ICUWB), 2014 IEEE International Conference on*, pages 280–285, Sep 2014.

[2] J. Tiemann, F. Schweikowski, and C. Wietfeld. Design of an UWB indoor-positioning system for UAV navigation in GNSS-denied environments. In *Indoor Positioning and Indoor Navigation (IPIN), 2015 International Conference on*, Oct 2015.

[3] F. Hartmann, F. Pistorius, A. Lauber, K. Hildenbrand, J. Becker, and W. Stork. Design of an embedded UWB hardware platform for navigation in GPS denied environments. In *Communications and Vehicular Technology in the Benelux (SCVT), 2015 IEEE Symposium on*, pages 1–6, Nov 2015.

[4] K. O’Keefe, Yuhang Jiang, and M. Petovello. An investigation of tightly-coupled UWB/low-cost GPS for vehicle-to-infrastructure relative positioning. In *Radar Conference, 2014 IEEE*, pages 1295–1300, May 2014.

[5] W. Chantaweesomboon, C. Suwatthikul, S. Manatrinon, K. Athikulwongse, K. Kaemarungsi, R. Ranron, and P. Suksompong. On performance study of UWB real time locating system. In *2016 7th International Conference of Information and Communication Technology for Embedded Systems (IC-ICTES)*, pages 19–24, Mar 2016.

[6] D. Neirynck, M. O’Duinn, and C. McElroy. Characterisation of the NLOS Performanceof an IEEE 802.15.4a Receiver. In *12th Workshop on Navigation, Positioning and Communications (WPNC15)*, May 2015.

[7] R. Dalce, A. van den Bossche, and T. Val. An experimental performance study of an original ranging protocol based on an IEEE 802.15.4a UWB testbed. In *2014 IEEE International Conference on Ultra-WideBand (ICUWB)*, pages 7–12, Sep 2014.

[8] H. Kim. Performance comparison of asynchronous ranging algorithms. In *Global Telecommunications Conference, 2009. GLOBECOM 2009. IEEE*, pages 1–6, Nov 2009.

[9] R. Dalce, A. van den Bossche, and T. Val. Reducing localisation overhead: A ranging protocol and an enhanced algorithm for uwb-based wsns. In *2015 IEEE 81st Vehicular Technology Conference (VTC Spring)*, pages 1–5, May 2015.

[10] Ubisense. Ubisense website. [Online]. Available: http://ubisense.net/, May 2016.

[11] H. Cho, Y. Jung, H. Choi, H. Jang, S. Son, and Y. Baek. Real time locating system for wireless networks using ieee 802.15.4 radio. In *2008 5th Annual IEEE Communications Society Conference on Sensor, Mesh and Ad Hoc Communications and Networks*, pages 578–580, Jun 2008.

[12] R. Hach and A. Rommel. Wireless synchronization in time difference of arrival based real time locating systems. In *Positioning Navigation and Communication (WPNC), 2012 9th Workshop on*, pages 193–195, Mar 2012.

[13] M. R. Gholami, S. Gezici, and E. G. Strom. TDOA based positioning in the presence of unknown clock skew. *IEEE Transactions on Communications*, 61(6):2522–2534, Jun 2013.

[14] C. McElroy, D. Neirynck, and M. McLaughlin. Comparison of Wireless Clock Synchronization Algorithms for Indoor Location Systems. In *Communications Workshops (ICC), 2014 IEEE International Conference on*, pages 157–162, Jun 2014.

[15] Alan Bensky. *Wireless Positioning Technologies and Applications*. The GNSS Technology and Applications Series. Artech House, Boston, Mass. [u.a.], 2008.

[16] IEEE Std 802.15.4-2011: Part 15.4: Low-Rate Wireless Personal Area Networks (LR-WPANs). http://standards.ieee.org/getieee802/download/802.15.4-2011.pdf.

[17] F. Eckermann and J. Tiemann. Raw dataset, http://dx.doi.org/10.5281/zenodo.51877. May 2016.

[18] Norman Abramson. The ALOHA system: Another alternative for computer communications. In *Proceedings of the November 17-19, 1970, Fall Joint Computer Conference*, AFIPS ’70 (Fall), pages 281–285.